

Structural and Magnetic Properties of Co-Cu Film Systems

A. R. Bachmann,¹ S. Speller,¹ J. Manske,¹ M. Schleberger,¹
A. Närmann,² and W. Heiland¹

¹*Fachbereich Physik,
Universität Osnabrück,
D-49069 Osnabrück,
GERMANY*

²*Physikalisches Institut,
Technische Universität Clausthal,
D-38678 Clausthal-Zellerfeld
GERMANY*

Abstract

Thin films of Co on Cu are studied with respect to structural and magnetic properties by means of STM, MOKE and spin sensitive electron capture from surfaces (ECS). Sub-monolayer coverages of Co have been deposited on vicinal Cu(111) surfaces with steps oriented along $\langle 1\bar{1}0 \rangle$. STM topographies revealed that on vicinal surfaces regular arrays of steps with $\{100\}$ as well as with $\{111\}$ minifacets can be prepared. As Co is deposited it aggregates on both types of surfaces at the steps. On the surfaces with the $\{100\}$ facets the step array is rearranged into a configuration where double steps dominate. Along the $\{100\}$ facets of the double steps the Co exists as one-dimensional structures. Magnetic properties, *e.g.* hysteresis loops, are measured for different Co thicknesses above one monolayer on low-indexed Cu(111). The difference between the ECS and the MOKE hysteresis loops, respectively, afford insights into relations between bulk and surface magnetic properties.

I. Introduction

On surfaces a wide range of nanosized low-dimensional structures can be realized. Especially structures of non-ferromagnetic combined with ferromagnetic materials are interesting for magnetoelectronics. Even more challenging is the production of one-dimensional structures which might exhibit totally different magnetic properties.¹ Vicinal surfaces often exhibit quite regular step arrangements and preferred aggregation

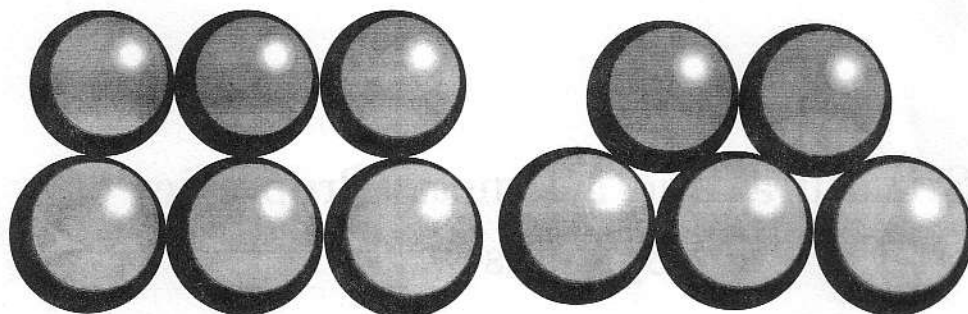


Figure 1. Sphere models of the $\{100\}$ and $\{111\}$ step facets

of ferromagnetic materials at steps has been observed for the systems Co/Cu(111),² Cr/Cu(111),³ and Ni/Ag(111).⁴ With sub-monolayer coverages of Co on Cu(111) approximately 50 Å wide decoration bands are formed along step edges.² Thicker films of Co on Cu(111) have been studied as well. For Co films between 1.5 and 15 monolayers a strong tendency for island formation is observed. The structure changes from face-centered-cubic to hexagonal at a film thickness of approximately 5-6 monolayers.⁵ Layer-by-layer growth may be achieved at very high deposition rates, as shown by Zheng *et al.*⁶ or by the use of Pb as a surfactant.⁷

In this study we used samples with narrow terraces, below 50 Å and coverages below 0.1 monolayer. With scanning tunneling microscopy (STM) we observe distinct morphologies upon Co deposition on vicinal Cu(111) surfaces with different step facet but identical step (edge) orientation. There are indications for one-dimensional alloying of Co in Cu steps with $\{100\}$ minifacets. Additionally, we have investigated the magnetic properties of thicker Co films on Cu(111) with ECS and MOKE.

II. Experiment

For the STM measurements we use an Omicron STM I setup, equipped with Auger electron spectroscopy (AES), low energy electron diffraction (LEED), and reflection high energy diffraction (RHEED). Cu(111) disks have been cut off by spark erosion from a monocrystalline Cu rod after alignment by Laue diffraction. The slices have been cut into two pieces along $\pm[\bar{1}10]$ and wedged using a polishing machine. The surfaces of the samples have been polished mechanically and electrochemically. The surfaces are vicinal to (111) and the 5° miscut is about the $[\bar{1}\bar{1}2]$ direction. Therefore, the steps run along the dense $\pm[\bar{1}10]$ directions and exhibit either exclusively $\{100\}$ -type or $\{111\}$ -type minifacets at the step edges (Fig. 1) depending on whether the miscut is clockwise or counterclockwise. The atomic spacing along the steps is $a_{\parallel} = 2.55$ Å and the spacing of the rows in the terrace perpendicular to the steps is $a_{\perp} = 2.21$ Å. The average terrace width of the 5° sample pair is 23.9 Å. Both samples of the pair were mounted together on the same holder. Between the back of the samples and the holder a roof was inserted in order to compensate for the wedge shape of the samples. With this mounting completely equal preparation conditions on both samples were achieved. Sputter-anneal cycles have been applied till a nice beam splitting in LEED patterns was observed as well as AES and STM cleanliness. Deposition of Co was done at room temperature using a thermal evaporator. STM images have been taken at room temperature using tungsten tips. The step type has been identified by Laue diffraction, LEED and atomically resolved STM images.

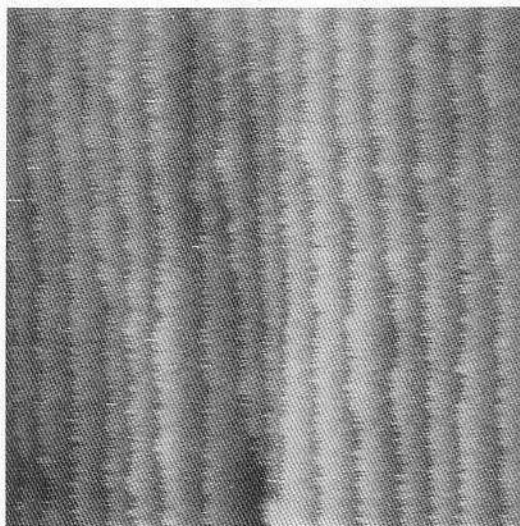


Figure 2. Cu(111) surface with 5° miscut and $\{100\}$ steps (380 Å, -2.3 V, 0.7 nA).

For the magnetic measurements, a low-indexed Cu(111) substrate was used. It was cut and prepared in the same way as the vicinal Cu(111) samples. We applied two methods, the magneto-optical Kerr effect (MOKE) and electron capture spectroscopy (ECS). The former is a standard tool and will not be described here (see *e.g.* Ref. 8, the latter is somewhat uncommon and will be briefly described in the following (for details see *e.g.* Ref. 9). The scattering of low energy He^+ -ions yields mostly neutralized ground state He atoms. But a fraction is neutralized into excited states. The subsequent deexcitation occurs via light emission. The electron spin is conserved during the neutralization process. Because of dipole selection rules, the information about the spin orientation is eventually transferred to the emitted photons. If the electrons at the surface have a netto spin polarization (*e.g.* at a magnetic surface) their spin has a preferred orientation. The magnetic sublevels of the He atom are occupied accordingly and the emitted light is circularly polarized. The sense of rotation and the degree of polarization are directly related to the spin polarization. Combining ion scattering and optical spectroscopy, we are thus able to obtain information about the surface magnetization. Recently, we could show that ECS is extremely surface sensitive and that it is possible to measure hysteresis loops.¹⁰

III. Results and Discussion

In Fig. 2 we show the typical STM topography of the vicinal surface as prepared prior to deposition. The surfaces with the $\{100\}$ steps and the $\{111\}$ steps appear qualitatively equal (except for atomic resolution). The steps arrange themselves in a regular array. Occasionally, impurities are visible which pin steps (see *e.g.* at the bottom center of Fig. 2). Apart from that no multiple steps are present. In STM images step edges appear frizzy, indicating kink mobility that is undersampled in time by the STM. Such a high mobility at ambient temperature is typical for materials with a relatively low melting point. Directly at the pin points the frizziness is absent. We found that the $\{111\}$ steps display stronger frizziness and wider terrace width distributions compared to $\{100\}$ steps and inferred different elastic step-step-interactions.¹¹

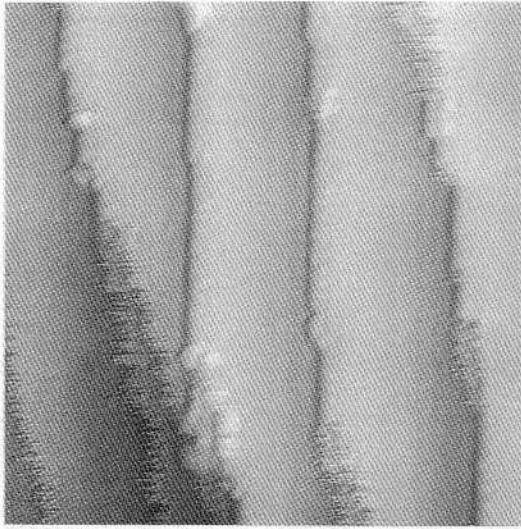


Figure 3. Cu(111) surface with 5° miscut, $\{100\}$ steps and low Co coverage. The 'beady' step edges contain Co and have double height (185 Å, -0.3 V, 0.7 nA).

After small amounts of Co have been deposited onto the vicinal surfaces the Co aggregates at both types of steps (Figs. 3 and 4). In this coverage and terrace width regime islands are almost never located on terraces. There are striking differences in the morphology of the two surfaces with respect to the step type. The most remarkable effect of the Co is that on the surfaces with the $\{100\}$ steps the step array is rearranged into a configuration where double steps prevail (Fig. 3). These rearrangements afford considerable mass transport in the substrate surface. These double steps do not display frizziness. Since according to AES no third element is present in the surface region we must attribute this to incorporated Co. The stronger binding immobilizes larger agglomerates of Co. Thus kink diffusion becomes slow compared to usual STM sampling rates of some kHz when Co is involved. In smaller STM frames the edges of the double steps appear corrugated (Fig. 3). The amplitude of this corrugation is 0.3 \AA and its periodicity is 5.1 \AA . This period is compatible with $2 \cdot a_{\parallel}$, the double atomic spacing of Cu(111) along $\langle 1\bar{1}0 \rangle$. Occasionally, single steps with fringes are found. The topography of these steps and the clean steps is the same and we conclude that they do not contain Co. We did not find any steps that are both single and without fringes nor did we find any frizzled steps of double height. The corrugation period and the lack of mobility suggest an arrangement of alternating Co and Cu atoms at the double step edges. The STM topographies do not allow to deduce the complete atomic arrangement of the Co atoms within the $\{100\}$ step in detail. The analysis of our data yields that the non-frizzy, double steps are always very accurately aligned with $\langle 1\bar{1}0 \rangle$ whereas monoatomic, frizzy steps can be misoriented by up to 30° . Misalignments are rarely observed with the clean steps of the uncovered surface. Thus, the misalignments occurring with Co coverage must be a consequence of the step pairing. It is instructive to look more closely at the transition zones between the double steps and single step pairs. Four of such transitions are visible in Fig. 3. This kind of transition resembles a zipper. The closed part of the zipper is represented by the double step which is always straight. The open part of the zipper is represented by two frizzy simple steps. This special configuration suggests that the formation process of the double steps works

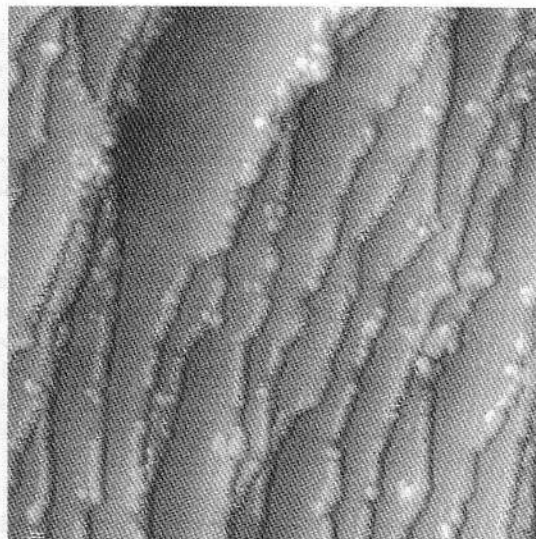


Figure 4. Cu(111) surface with 5° miscut, $\{111\}$ steps and low Co coverage. At the step edges there are islands and noisy bands present (380 Å, -2.2 V, 0.5 nA).

zipper-like as well. It is likely that Co atoms diffuse towards such transition points, are bound there and the two Cu steps arrange themselves in line with the 'closed' part of the zipper. In this way, the zipper can close more and more till the step misalignments in the open part are maximal.

In the topography of the surfaces with the steps of the $\{111\}$ type two major changes can be observed after the deposition (Fig. 4). First, islands of approximately 8 Å in diameter and of monoatomic height with respect to the higher terrace are present at steps, and secondly the regularity of the step array is reduced compared to the clean state (see Fig. 4). But unlike the steps with $\{100\}$ facets these steps are single steps and the mass transport is moderate. A new type of frizziness is observed along the step edges in between the islands (Fig. 4). The difference compared to the usual frizziness of clean step edges is that here the height is affected as well in an approximately 6 Å wide region. Thus, this new kind of frizzes extends parallel and perpendicular to the surface. The mean level the height fluctuates about is approximately 0.4 Å above the upper terrace. Since the width is very similar to the width of the islands we suspect behind these noisy bands small mobile Co agglomerates or an electronic effect of Cu kinks diffusing in front of embedded Co structures. As the coverage is increased this effect disappears.

The formation of double steps requires a high mobility on the surface and is actuated by the presence of Co atoms on the surface. Without Co there was no evidence for step doubling in our data. Step doubling represents a mechanism to reduce step-step-repulsion since in most cases this depends on the distance x as $1/x^2$. Molecular dynamics studies of clean vicinal Cu(111) surfaces yielded similar surface energies for single, double and triple steps when the step minifacet is $\{100\}$.¹² With $\{111\}$ -type steps surfaces with single steps turned out to be more stable than with multiple steps. This result is applied to clean steps. On the other hand, double steps are common in chemically ordered alloys when stacking of layers with alternating composition is present such as Pt₃Sn(100)¹³ and Cu₃Pd(110).¹⁴

Since double steps have double{100} minifacets their formation might be related with the situation on Cu(100) where site exchanges are prevalent. It is helpful to compare with the Co structures found on flat Cu{100} and Cu{111}. Because of the larger surface energy of Co it is unfavorable that the Co stays exposed to the vacuum. With both substrate orientations a certain degree of encapsulation or embedding of the Co by Cu was observed. On Cu(111) a partial capping or replacement of the Co islands by substrate material was found.^{2,5,15} On Cu(100) there are indirect indications of strong intermixing after annealing.^{16,17} In STM topographies, the apparent height of small Co islands on Cu(100) depended on the gap voltage which is rather unusual for metallic systems.¹⁷ This finding points towards a change in the electronic structure, possibly a consequence of surface intermixing or even alloying. According to an STM and a density-functional theory study Co occupies substitutional sites in the Cu(100) substrate.¹⁸ The exchanged Cu atoms form larger islands on the surface and become decorated by Co. These results are helpful to interpret our findings. The islands on the vicinal Cu(111) surface with the {111} step facets are not surprising, since they are similar to the islands at the steps of the flat surfaces. Considering, that for the capping of the islands substrate material is removed, also the decrease of the step regularity of the vicinal surface must be expected when Co islands are present. On Cu(111) substrate damages have been observed in form of circular vacancy islands.^{2,5,15} At ambient temperatures this so called etching is not saturating within reasonable times scales.¹⁹ At the Co islands the steps are pinned and thus the etching must be stronger at uncovered step regions further away from islands. The step etching is therefore highly non-uniform. The reduction of the step regularity observed on the vicinal surface with {111} step facets and Co islands is in line with these results. On the surface with the {100} steps site exchanges are likely to occur when Co atoms reach the {100} minifacets. Since the minifacets exist only along the step lines one-dimensional Co structures result. Thereby, substrate atoms are released which are supposed to attach to the steps of the open part of the zipper.

We did not investigate films in the sub-monolayer range by ECS since the Co-Cu(111) system is too volatile. The additional energy of the impinging ion beam is already sufficient to give rise to a substantial intermixing of the surface layers. A decrease of the Co/Cu ratio in the topmost layer on a time scale of hours has already been observed by low-energy-ion scattering for Co/Cu(111).²⁰ Thus, very thin films of Co on low-indexed Cu(111) are unstable and Co is removed efficiently out of the top layer by the ion beam. This was further substantiated from our Auger-measurements as well as from our ECS experiments. We estimate the life-time of one monolayer Co on top of a Cu(111) surface under ion bombardment to be around the order of minutes. For MOKE measurements, the signal stemming from a sub-monolayer coverage is too small to be quantitatively analyzed with the present setup. Therefore we investigate the magnetic properties of Co films between one and twenty monolayers. In this range the films are sufficiently thick so that we are able to record hysteresis loops with ECS without destroying the film under investigation.

Figure 5 shows the magnetic ECS signal from a clean Cu(111) surface. The circular polarization $-S/I$ is stable around 40% independent of the magnetizing current. This clearly shows that at the Cu(111) surface no spin-polarization exists. That changes drastically if we deposit 6 monolayers of Co on top of the Cu(111) surface. As shown in Fig. 6, the surface now responds to the magnetizing field. A hysteresis is observed that is clear evidence for the ferromagnetic order of the topmost layer. For comparison we have included the hysteresis that we obtained from the same system by means of MOKE. Neither MOKE nor ECS data yield quantitative information about the

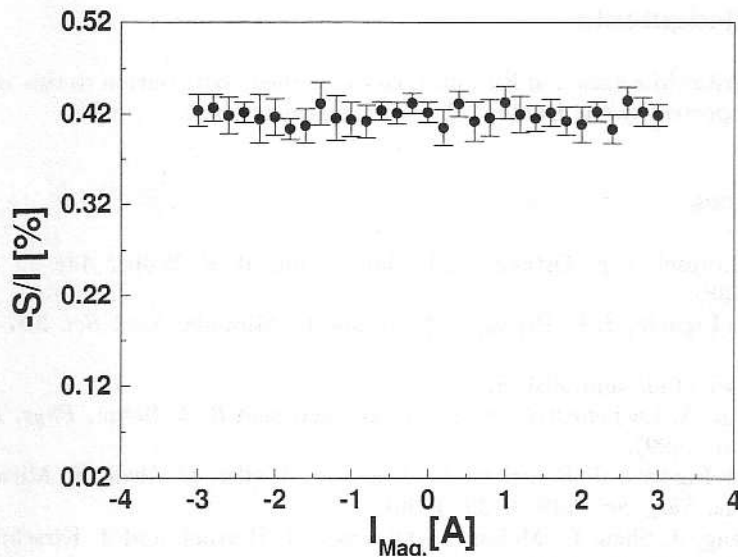


Figure 5. Circular polarization from a clean Cu(111) sample as a function of the applied magnetic field. Primary energy $E_P = 10$ keV, angle of incidence $\Psi = 3^\circ$.

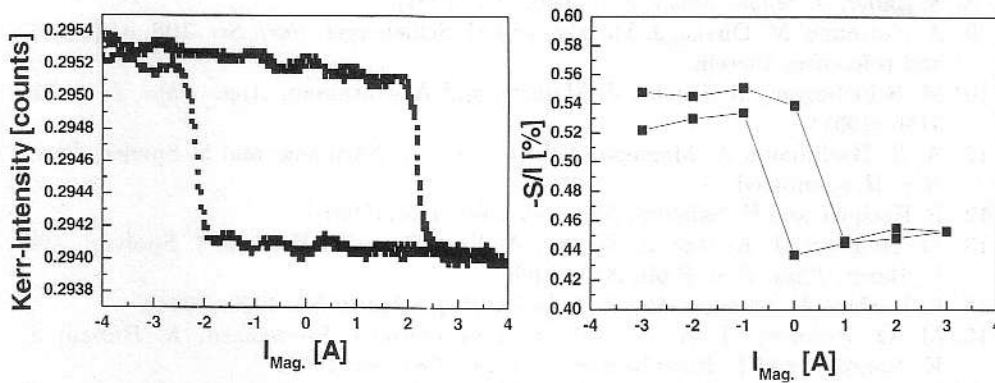


Figure 6. Hystereses of 6 monolayers Co/Cu(111) measured with MOKE (right panel) and with ECS (left panel). The oscillations seen in the MOKE hysteresis are due to our experimental setup.

magnetic moment but the difference in the coercivity of the hystereses is obvious from Fig. 6. This is clear evidence that the magnetic behaviour at the very surface of the system is intrinsically different from the bulk. From several experiments with different Co film thicknesses we conclude that the magnetization signal at first increases linearly with the film thickness and then saturates at a thickness of $\simeq 6$ –8 monolayers. This could be due to a change of the geometrical structure^{5,21} and/or a change of the magnetic structure (in-plane to off-plane²²) of the topmost layer. To establish the precise dependence of the magnetization signal as a function of the Co film thickness and of the film structure more data is required which will be acquired in future experiments.

Acknowledgments

We thank Aitor Murgaza and Enrique Ortega for their contribution to this work. This work is supported by the Deutsche Forschungsgemeinschaft.

References

1. F. J. Himpsel, J. E. Ortega, G. J. Mankey, and R. F. Willis, *Adv. in Phys.* **47**, 511 (1998).
2. J. de la Figuera, J. E. Prieto, C. Ocal, and R. Miranda, *Surf. Sci.* **307-309**, 538 (1994).
3. S. Speller *et al.*, unpublished.
4. S. Morin, A. Lachenwitzer, O. M. Magnussen, and R. J. Behm, *Phys. Rev. Lett.* **83**, 5066 (1999).
5. J. de la Figuera, J. E. Prieto, G. Koska, S. Müller, C. Ocal, R. Miranda, and K. Heinz, *Surf. Sci.* **349**, L139 (1996).
6. M. Zheng, J. Shen, C. Mohan, P. Ohresser, J. Barthel, and J. Kirschner, *Appl. Phys. Lett.* **74**, 425 (1999).
7. W. Kuch, A. Dittshar, M.-T. Lin, M. Salvietti, M. Zharnikov, C. M. Schneider, J. Kirschner, J. Camarero, J. J. de Miguel, and R. Miranda, *J. Magn. Magn. Mat.* **170**, L13 (1997).
8. S. Bader, *J. Magn. Magn. Mat.* **100**, 400 (1991).
9. A. Nürmann, M. Dirska, J. Manske, and M. Schleberger, *Surf. Sci.* **398**, 84 (1998), and references therein.
10. M. Schleberger, M. Dirska, J. Manske, and A. Nürmann, *Appl. Phys. Lett.* **71**, 3156 (1997).
11. A. R. Bachmann, A. Murgaza, J. E. Ortega, A. Nürmann, and S. Speller, *Phys. Rev. B*, submitted.
12. P. Hecquet and B. Salanon, *Surf. Sci.* **366**, 415 (1996).
13. M. Hoheisel, J. Kuntze, S. Speller, A. Postnikov, W. Heiland, I. Spolveri, and U. Bardi, *Phys. Rev. B* **60**, 2033 (1999).
14. L. Barbier, B. Salanon, and A. Loiseau, *Phys. Rev. B* **50**, 4929 (1994).
15. M. O. Pedersen, I. A. Bönicke, E. Lægsgaard, I. Stensgaard, A. Ruban, J. K. Nørskov, and F. Besenbacher, *Surf. Sci.* **387**, 86 (1997).
16. U. Ramsperger, A. Vaterlaus, P. Pfäffli, U. Maier, and D. Pescia, *Phys. Rev. B* **53**, 8001 (1996).
17. J. Fassbender, R. Allenspach, and U. Dürig, *Surf. Sci.* **383**, L742 (1997).
18. F. Nouvertné, U. May, M. Bammig, A. Rampe, U. Korte, G. Güntherodt, R. Pentcheva, and M. Scheffler, *Phys. Rev. B* **60**, 14382 (1999).
19. S. Speller, S. Degroote, J. Dekoster, G. Langouche, J. E. Ortega, and A. Nürmann, *Surf. Sci. Lett.* **405**, 542 (1998).
20. A. Rabe, N. Memmel, A. Steltenpohl, and T. Fauster, *Phys. Rev. Lett.* **73**, 2448 (1994).
21. S. Müller, G. Kostka, T. Schäfer, J. de la Figuera, J. E. Prieto, C. Ocal, R. Miranda, K. Heinz, and K. Müller, *Surf. Sci.* **352**, (1996).
22. W. Kuch, A. Dittshar, M. Salvietti, M.-T. Lin, M. Zharnikov, C. M. Schneider, J. Camarero, J. J. de Miguel, R. Miranda, and J. Kirschner, *Phys. Rev. B* **57**, 5340 (1998).